Diabetic Retinopathy: Severity Level Classification based on Object Detection (Microaneurysms, Hemorrhages, and Hard Exudates) using Mathematical Morphology and Neural Networks

Fifi Diah Rosalina[1], Dian C. Rini Novitasari[1], Ahmad Hanif Asyhar[1], Abdulloh Hamid[1], Muhammad Firmansjah[2]

[1]*Department of mathematics, UIN Sunan Ampel, Surabaya, Indonesia*

[5]*Departement of medical eye, Airlangga University, Surabaya, Indonesia*

Keywords : Diabetic retinopathy, Mathematical morphology, morphology reconstruction, backpropagation

Abstract : According to WHO, the number of people with diabetes had reached approximately 422 million people in 2014. Most cases of diabetes in the world occur as type 2 diabetes which can result in serious complications of vital organs such as the eyes, kidneys, and heart, causing death. Complications of diabetes often causes people with Diabetic Retinopathy (DR) to be unaware of the disease for several years, which can lead to permanent blindness. Early detection of DR is indicated by the presence of microaneurysms, bleeding, and hard exudates. Five DR severity classifications which include normal, mild-NPDR, moderate-NPDR, severe-NPDR and proliferative DR are performed using the backpropagation method. Detection methods for microaneurysms and hemorrhages are based on diamond disc and morphology opening methods, while detection of hard exudate features is based on morphology reconstruction methods and minimal area of images. The area and perimeter of each feature is applied as a backpropagation input with 80% of training data and 20% of test data from the total of 53 image data. Four inputs with 150 hidden layers are arranged as a network structure capable of producing MSE values of 0.000190 and an accuracy rate of 90.90%.

1. INTRODUCTION

The non-communicable disease of Diabetes Mellitus (DM) is one of the highest causes of death in the world. DM has received special attention from the World Health Organization (WHO) which proclaims sustainable development on the 2030 agenda. Sustainable development is aimed at reducing the mortality rate of 1.5 million deaths that occurred in 2012 and it is estimated that approximately 422 million adults in 2014 suffered from diabetes globally (WHO, 2016). Additionally, WHO states that DM can lead to various serious complications that can attack a number of vital organs which can lead to heart attack, stroke, kidney failure, leg amputation, vision loss, nerve damage and fetal death in pregnant women. Diabetes belongs to a group of metabolic diseases characterized by hyperglycemia due to damage to insulin secretion, insulin reaction, or both (American Diabetes Assosiation, 2010). Diabetes is divided into 2 types, the first is 1 diabetes (T1D), which occurs when the immune system has severe damage in the endocrine pancreatic beta cells that causes the hormone insulin to be deficient in vitamins (Stitt, et al., 2015). However, according to (WHO, 2016) the exact cause of type 1 diabetes is unknown and cannot be prevented, hence type 1 diabetics cannot survive without insulin. Type 2 diabetes (T2D) according to (WHO, 2016) is caused by abnormal pancreatic conditions that cannot produce the insulin hormone to control blood sugar levels. This disease may be left undiagnosed for several years because the symptoms are less marked, resulting in worsening complications. The majority of diabetics in the world are type 2 diabetes. T2D complications include DR due to abnormalities in the eye (Manullang, et al., 2015) where the eye blood vessels lack oxygen and cause nerve swelling in the retinal nerve (Yun, et al., 2008).

Early detection for DR identification can be performed by detecting microaneurysms, bleeding, and features of hard exudates. The study by Neera Singh and Ramesh Chandra Tripathi on automatic

Rosalina, F., Novitasari, D., Asyhar, A., Hamid, A. and Firmansjah, M.
Diabetic Retinopathy: Severity Level Classification based on Object Detection (Microaneurysms, Hemorrhages, and Hard Exudates) using Mathematical Morphology and Neural Networks.
DOI: 10.5220/0008906300002481
In *Proceedings of the Built Environment, Science and Technology International Conference (BEST ICON 2018)*, pages 272-280
ISBN: 978-989-758-414-5

early detection of diabetic retinopathy using image analysis techniques applied the concepts of mathematical morphology and fuzzy grouping methods to obtain feature extraction from nerves in the retina (Singh & Tripathi, 2010).

This research guideline by the author was based on two studies. The first study was the identification of the different stages of diabetic retinopathy using retinal optical images with the application of the backpropagation method. The four classifications of DR are: normal, severe NPDR, moderate NPDR and proliferative DR, which was able to produce sensitivity values of 91.7% and specificity of 100% and also predictive accuracy up to 84% (Yun, et al., 2008). The second study was carried out by Handayani Tjandrasa et al on the classification of non-proliferative diabetic retinopathy based on hard exudate using soft margin SVM with a segmentation process that gives good results of hard exudate segmentation (Tjandrasa, et al., 2013).

Based on the results of studies by Handayani Tjandrasa on good segmentation on the identification of hard exudates, and Wong Li Yun which was able to provide predictive results of 84% using the backpropagation classification, the title of this research is "The Classification of Severity of Diabetic Retinopathy based on Object Detection (Microaneurysms, Hemorrhages, and Hard Exudates) using Mathematical Morphology and Backpropagation". The two focus points in this study are the emergence of DR objects into five classifications. The five classifications include mild Non-Proliferative Diabetic Retinopathy (mild NPDR), moderate Non-Proliferative Diabetic Retinopathy (moderate-NPDR), Severe Non-Proliferative Diabetic Retinopathy (severe-NPDR), and Proliferative. The second point is the application of the backpropagation classification method. The results of the feature extraction values are applied as input to the backpropagation method as the value of the area and perimeter object.

2. COMPUTATIONAL METHOD AND THEORY

2.1 Diabetic Retinopathy (DR)

DR will appear as a long-term risk due to pancreatic conditions that are not able to control the sugar levels in the blood which is circulated as a source of energy for cells. If there is a large consumption of carbohydrates in the body while the insulin hormone that controls blood sugar levels cannot be produced properly, there will be a buildup of glucose in the blood that will increase in the eye's blood vessels. The appearance of microaneurysms, hemorrhages, and hard exudates can disturb the oxygen supply which will cause signs of ischemia or lack of oxygen in the blood vessels of the eyes and cause bleeding. The identification of the appearance of microaneurysms is the first sign of DR. This condition can develop into bleeding which is marked by the appearance of hard exudates until the growth of new blood vessels is fast and brittle.

On a global scale, patients with DR are classified into two types: NPDR and PDR. Whereas in this study the two types of DR were divided into five levels, as shown on Figure 2.1 (Dedeh, 2016). The five levels of the DR are described as follows (Yun, et al., 2008):

a. Normal: eye conditions are not impaired and are functioning well so the normal eye structure does not contain microaneurysms, bleeding or hard exudates.
b. Mild-NPDR: at this stage, there will be a small swelling in the retinal microvascular, called a microaneurysm. Accuracy in detecting the appearance of microaneurysms is a critical step that determines the initial identification of DR because the first abnormal condition that occurs in the structure of the eye is the appearance of microaneurysms (Dedeh, 2016).

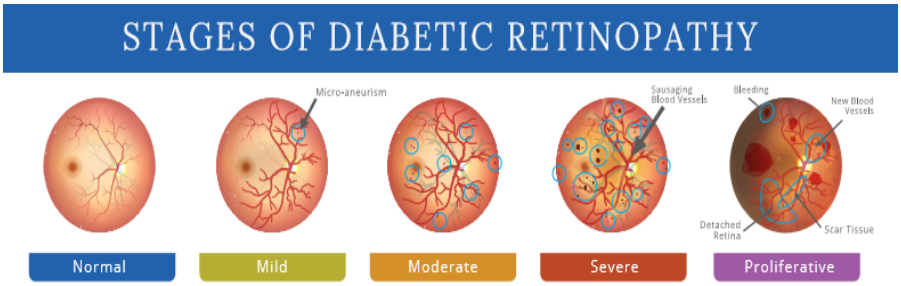

Figure 1: Stages of DR

c. Severe NPDR: the number of microaneurysms are rising, which causes the retinal area to lose blood supply and cause signs of ischemia such as bleeding. This stage is marked by the presence of hard exudates.
d. PDR: this stage is the advanced stage of the DR which is characterized by vasoproliferative results from the retina which causes abnormal and brittle growth of new blood vessels.

2.2 Adaptive Histogram Equalization (AHE)

The histogram is a graphical display that is used to show the distribution of data visually or how often different values occur in a dataset (Kho, 2018). The histogram provides information about variations in the process and helps management in making decisions as an effort to improve the sustainable process (Murinto, et al., 2008). The image is considered great if the gray level region has even distribution on each pixel intensity value. To increase image contrast from a small object texture, the AHE method is applied to improve image quality to increase the portion of the texture for the image (Hadinegoro, et al., 2012).

Adaptive Histogram Equalization (AHE) is a development of improved HE quality introduced by Pizer (1987) that is applied to natural images and medical images to provide better object clarity (Lusiana, et al., 2014). The HE method will calculate histogram equalization once for all images on each block, then the AHE method for histogram equalization is done several times for each block of n × n image. The calculation for each image block is solved by the following equation 1 to 3 (Woods, et al., 2004).

$$P_r(r_k) = \frac{n_k}{n}, and\ r_k = \frac{k}{L} \quad (1)$$

$$S_k = T(r_k) = \sum_{j=0}^{k} P_r(r_j) \quad (2)$$

$$= \sum_{j=0}^{k} \frac{n_j}{n} \qquad k = 0,1,2,\dots,L-1$$

$$S_k = s_k + P_r(r_k) \quad (3)$$

where :
k : Range of gray degrees
L : The biggest gray level
r_k : Average of initial gray level
$P_r(r_k)$: Initialization of the histogram
n_k: Amount of all pixels
S_k : Average gray level (cumulative frequency)
$P_s(S_k)$: Result of equalization histogram

2.3 Morphology Opening

Morphology operation is the process of modification of each point that corresponds to the modification of the object being observed, or is an operation based on a segment or part in the image that becomes the focus of attention (Ekanita, 2004). Element structure in morphology operations is the basis for determining the accuracy of the results of object recognition in the image. Element structure is defined as a set of small sub-images that are used to recognize object shapes in the image (Prasetyo, 2012).

Opening is an erosion process followed by dilation. It is usually used to eliminate noise, make the object boundary smoother, and be able to maintain the size of the object with the actual size. Erosion is a technique of reducing or eroding the edge of an object with the calculation shown in Equation 4.

$$A \ominus B = \{x \in E^N | x + b \in A \text{ for } b \in B\} \quad (4)$$

Dilatation is the opposite of erosion operations, namely the technique of enlarging an image object by adding layers around an object using the calculation shown in Equation 5.

$$A \oplus B = \{c \in E^N | c = a + b, a \in A, b \in B\} \quad (5)$$

Where :
A :State of the set of binary image elements, namely the N dimension in black and white
B : Another set of binary image elements, namely the N dimension in black and white
E^N:Vector set (coordinates) in Euclid space E^N

2.4 Morphology Reconstruction

Morphology reconstruction is a segmentation process to distinguish objects observed with other objects. Reconstruction is defined as the transformation of the learning structure or form of objects based on two images together with one element structure (Prasetyo, 2012). The two images are a starting point or marker in the transformation process. Another image is a mask or cover to resolve the constraints of the transformation process. The element structure applies to define connectivity for two images as a reconstruction process.

The image as a mask is symbolized as g and f as a marker in which morphology reconstruction g from f as $R_g(f)$ is defined by the steps in the following equation (Prasetyo, 2012).

a. Initialization of h_1 as an image marker$f$
b. Specify the structure of element B to be applied
c. Repeat the calculation of Equation 6

$$h_{k+1} = (h_k \oplus B) \cap g \quad (6)$$

d. Until the results are obtained like Equation 7

$$h_{k+1} = h_k \quad (7)$$

Mask of g must contain markers of f or image of marker f must be part of g, which is defined by Equation 8

$$f \subseteq g \quad (8)$$

The accuracy in determining the image that applies as a mask and marker in binary or grayscale images plays an important role in the results obtained from the morphology reconstruction process on two different images.

2.5 Backpropagation

The structure of the neural backpropagation network has a training process to balance the network's ability to recognize the patterns used during training. The backpropagation method is able to provide the right response to input patterns with training patterns, so that weighting is carried out in the training process as a digging factor from other input patterns. The steps of the backpropagation algorithm are resolved as follows:

a. Network Initialization (determines the activation function)

$$f(x) = \frac{2}{1 + e^{-x}} - 1 \quad (9)$$

b. Progressive propagation

1. Sum weight bias signal and the input value in the hidden layer unit

$$Z_{net\ j} = v_{j0} + \sum_{i=1}^{n} x_i v_{ji} \quad (10)$$

$$Z_j = f(Z_{net\ j}) \quad (11)$$

Then dispatch the signal to all output units.

1. Each output unit Y_k sum the weight of the input signal to the output node

$$y\_net_k = w_{k0} + \sum_{j=1}^{p} z_j w_{kj} \quad (12)$$

$$y_k = f(y\_net_k) \quad (13)$$

c. backward propagation

1) Each unit of output Yk receives a target pattern according to the pattern of training inputs and calculates an error value

$$\delta_k = (t_k - y_k) f'(y\_net_k) \quad (14)$$
$$= (t_k - y_k) y_k (1 - y_k)$$

Calculation of correlation weighting and calculation of bias correction

$$\Delta w_{kj} = \alpha \delta_k z_j \quad (15)$$

$$\Delta w_{0k} = \alpha \delta_k \quad (16)$$

2) Add the delta input based on the errors in each hidden unit to calculate the error factor δ

$$\delta\_net_j = \sum_{k=1}^{m} \delta_k w_{kj} \quad (17)$$

$$\delta_j = \delta_{\_net_j} f'\left(z\_net_j\right) = \delta_{net z_j (1 - z_j)} \quad (18)$$

Calculate the weight correction using

$$\Delta v_{ji} = \alpha \delta_j x_i \quad (19)$$

And calculate the correction bias with

$$\Delta v_{0j} = \alpha \delta_j \quad (20)$$

d. Weight changes

1) Weight changes of Y_k and bias j

$$w_{kj}(new) = w_{kj}\ (out) + \Delta w_{kj} \quad (21)$$

Change the weight of each hidden unit z_j and bias

$$v_{ji}(baru) = v_{ji}\ (lama) + \Delta v_{ji} \quad (22)$$

2.6 Mean Square Error (MSE)

Mean Square Error (MSE) is a method that can be used to evaluate the overall error rate of the output value of the target value. MSE is the average value that is obtained by summing all errors from the difference in target value and output value.

The application of MSE in this study is used to see the error rate of output values and targets of the image classification used in training data. This happens as a process of building a backpropagation structure for the classification of diabetic retinopathy images that have been validated at the Dr. Soetomo Hospital before finally being applied to the testing data.

The target classification value of the training data is guided by the binary code in Table 2, which consists of binary code for the classification of normal to proliferative images. If the MSE obtained from the training process gives the smallest possible value, it can be interpreted that the error rate of the output value with the target value towards the point of error is minimal.

The smallest MSE value may indicate the amount of training data that was correctly classified, so that the best weighted stored can be applied to test the classification of diabetic retinopathy images in testing data.

3. RESEARCH METHOD

3.1 Data

The data used in this study were fundus images obtained from the DIARETDB website and validated by the ophthalmologist at Airlangga University. Digital image data used in training and testing amounted to 53 data where 80% of the data was used in the training process, with 42 data used to obtain the pattern in the classification process. 20% of the data was tested with 11 image data to test the accuracy of the designed system. The process of testing the

classification of the severity of DR was from the data images of normal retinal conditions to those with diabetic proliferative retinopathy or rise of swelling and bleeding in the eye's nerves. The data was then entered into five stages in a flexible image format and was usually stored as 8 bits or 16 bits of each color R, G, B.

3.2 Identification of Hemorrhages and Hard Exudates

The identification of the three objects in this study had different image properties. The image processing carried out in this study was divided into two segmentation processes. The first process was carried out using opening morphology surgery for the identification of microaneurysms and hemorrhages. The second process applied morphology reconstruction methods and minimal areas of imagery that were applied to identify hard exudates. In general, the completion algorithm for both processes is shown on Figure 2.

3.3 Pre-Processing Images

The fundus image that was applied as input was an RGB type image with a .tif data format. Resizing was done due to the fundus image data having different pixel sizes, so if it is still done then the calculation of the area and perimeter values of the object would not be equal. The level of object clarity on pre-processing affects the segmentation process in distinguishing objects from other objects.

3.4 Segmentation of Microaneurysms and Hemorrhages

The two opening operation processes were reduced to provide better clarity on the edges of the object and binarized to obtain segmentation results in black and white. A white image indicates the object being observed, while black indicates the background of the image. The area and perimeter values from the results of this segmentation feature extraction processes that apply as input to the backpropagation structure.

3.5 Segmentation of Hard Exudates

Image segmentation was used to identify hard exudates based on the morphology reconstruction methods from the two images. Two selected images contributed to the accuracy of the segmentation results obtained. The image acting as a marker was an image of the contrast improvement effect using AHE, while the image that acts as a mask is the image of the result of erosion. After the segmentation process was carried out, the area and perimeter values of the segmentation results apply as input to the backpropagation method.

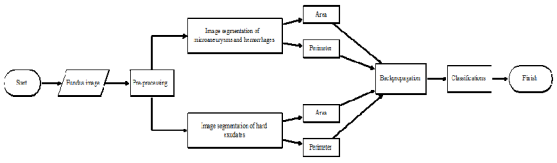

Figure 2: Flowchart of the identification of microaneurysms, hemorrhages, and hard exudates

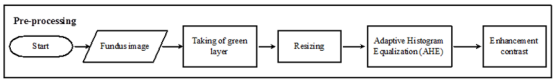

Figure 3: Flowchart of pre-processing images

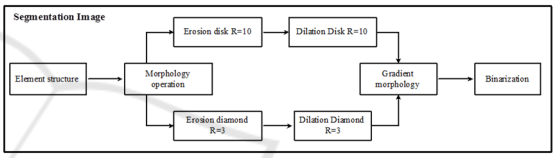

Figure 4: Flowchart of segmentation microaneurysms and hemorrhages

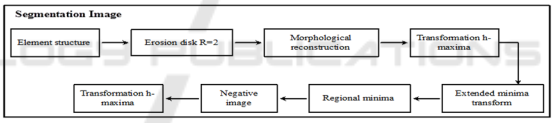

Figure 5: Flowchart segmentation of hard exudates

3.6 Classifications of Backpropagation

The backpropagation method is applied to study the input pattern and the intended target based on the number of hidden layers, learning rate, and the number of iterations that have been determined.

Quantization of area features and perimeter microaneurysm extractions, hemorrhages, and hard exudates was applied as input with a number of five outputs as shown on Figure 6. A decision was made from the results of classification of the backpropagation and built with the binary code that determined the five classifications of DR.

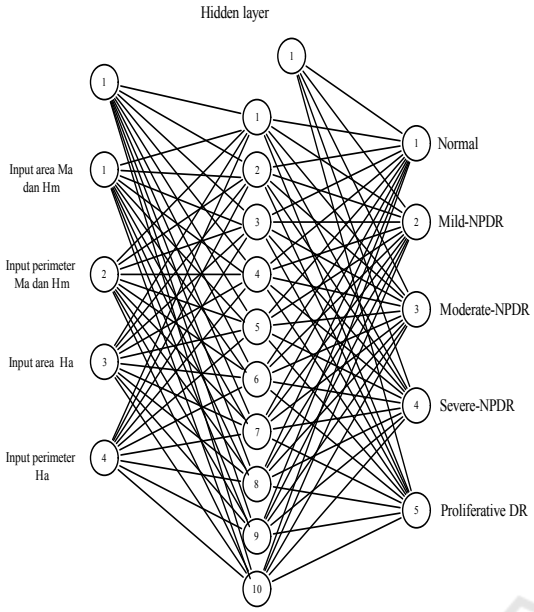

Figure 6: Structure of backpropagation classification

4. RESULTS AND DISCUSSION

The results were segmented based on the stages in Figure 4 based on the extraction of area features and perimeter of the microaneurysm objects, hemorrhages, and eye blood vessels. This condition occurs because the eye blood vessels were not eliminated in the segmentation process due to requiring additional methods. Microaneurysms, hemorrhages, and eye blood vessels were calculated as area values and perimeter objects were applied to the backpropagation input.

Figure 7: Original images of identification of micro-aneurysms and hemorrhages

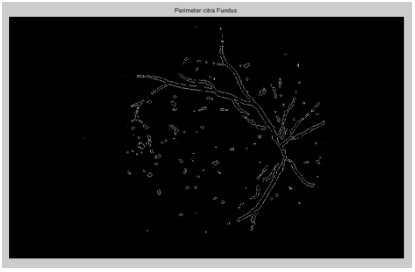

Figure 8: Perimeter identification of microaneurysms and hemorrhages

The identification process of hard exudates was then carried out to detect the existence of hard exudates. Pre-processing was carried out in the same way as the detection of microaneurysms and hemorrhages because the initial results and image quality improvement can provide better results to show hard exudates. However, the segmentation process was carried out using morphology reconstruction methods and a minimum area of image that separates hard exudates into black levels.

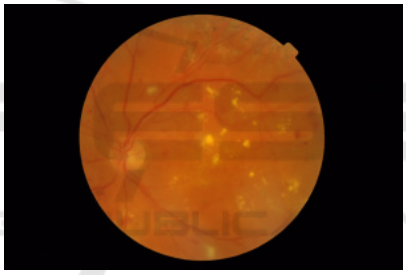

Figure 9: Original images of the identification of hard exudates

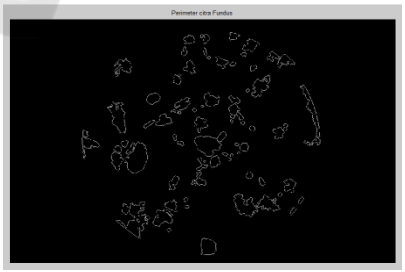

Figure 10: Perimeter of the identification of hard exudates

The segmentation process of hard exudates in Figure 10 provides identification with great results for the identification of small objects. Optical disks that have the same color intensity as hard exudates are segmented as observed objects because the elimination of optical disk is not performed because it requires additional methods. This condition will

certainly bring the area and perimeter of the hard exudates. A comparison between hard exudates with the initial image can be seen on Figure 10.

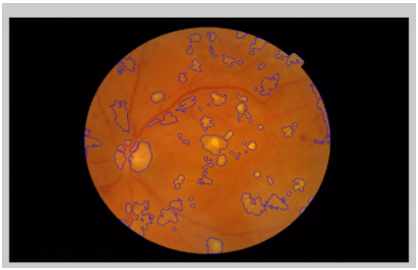

Figure 11: Perimeter of the hard exudates in the original image

The number of transformations of the hidden layers and LR values are applied as guidelines to obtain the best pattern recognition generated from the specified backpropagation structure. The backpropagation structure and results of the training and testing processes of the three objects are identified for the five classifications, as shown on Table 1.

From the the results of training and testing in Table 1, it can be concluded that the more hidden layers are used, the error value obtained from the training results will also be smaller, but a small error value of the training results does not always determine that the results of testing accuracy are getting better.

Furthermore, the preparation of backpropagation structures of different LR and HL values of 25 to 150 show different MSE results. Table 1 provides an explanation that the smaller LR value in the backpropagation structure learning process towards the specified target value (binary code in Table 2) can produce a smaller MSE value, where at LR 0.1 the largest accuracy value was 54.55%, LR 0.01 was 72.72% and the smallest LR 0,001 was given accuracy to 90.90%. The smaller the LR value and the greater the number of HL, the better the learning process of the target value can be implied to the small error value and the opportunity to attain better accuracy.

The accuracy values in Table 1 represent the number of testing data that was correctly classified from all 11 testing data. The magnitude of the accuracy value obtained shows that more and more testing images were correctly classified.

Table 1: Training and testing of the five classifications

Data training (80%)	Data testing (20%)	LR	HL	MSE	Accuracy (%)
42 data	11 data	0,1	25	0,0901	45,45
			50	0,0410	45,45
			75	0,0288	45,45
			100	0,0281	45,45
			125	0,00683	54,55
			150	0,000783	54,55
		0,01	50	0,0326	45,45
			75	0,00756	45,45
			100	0,00305	72,72
			125	0,00397	45,45
			150	0,000792	54,54
		0,001	25	0,0854	36,36
			75	0,00826	36,36
			100	0,00405	45,45
			125	0,0205	72,72
			150	0,000190	90,90

Image classification from the results of the training and testing of backpropagation structures resulted in a total output of five and was determined based on binary code. The binary code that was formed for the classification of the five levels of severity is shown on Table 2. The binary code was applied as a target of the backpropagation structure that resulted in the five different output values. The largest backpropagation output value is represented by the binary code 1, while the other is 0, so that the numbers 1 and 0 represent the results of certain classifications of the tested image.

Table 2: Binary code

	Binary code				
Mild-NPDR	1	0	0	0	0
Moderate-NPDR	0	1	0	0	0
Normal	0	0	1	0	0
Proliferative	0	0	0	1	0
Severe-NPDR	0	0	0	0	1

The percentage of the correctness level of the DR severity classification was obtained by dividing the classified data by the total number of tested images. The best accuracy results based on Table 1 were formed in the backpropagation structure of LR 0.001, HL of the amount of 150 with MSE of 0.000190 and an accuracy of 90.90%.

The results of the backpropagation classification on 11 data testings resulted in 10 data that was classified correctly and 1 data that was classified incorrectly. True classified images include two mild-

NPDR images, 3 moderate-NPDR images, one normal image, two proliferative images, and 2 images of severe-NPDR.

Area and perimeter values from feature extraction that were applied as backpropagation inputs allowed mild classes to enter the range value of moderate classes. This condition also occured in the classes from other classifications. Several studies on the classification or identification of many DR complications tend to focus on one type of object such as microaneurysms or hard exudates. If the DR severity classification was based on the three objects as in this study, the segment will only produce objects that are detected without involving optical disks, eye veins and other objects that were not observed. From the classification process, only results in the observed object segmentation of DR severity will achieve the best results.

The best process of image processing to produce object segmentation was determined by the accuracy of the classification results and was built on the backpropagation structure which impacted the size of the MSE value and the value of accuracy. As observed on Table 1, the smaller MSE values tend to produce better accuracy values, but also depend on the value of the feature extraction area and perimeter which was applied as input for the classification of the severity of diabetic retinopathy. This allows MSE training results with a small value, but results in a test accuracy value that is not large enough; this condition is influenced by each image data which has different lighting, image contrast, image structure to the level of clarity of different objects.

5. CONCLUSION

Based on the identification of microaneurysms, hemorrhages and hard exudates, the classification of the three objects according to the five severity levels of DR is described as the following three points:

1. The disk mathematical morphology method of $R = 10$ and diamond of $R = 3$ can be applied to visualize the object being observed with the background of the image
2. The hard exudates segmentation in this study resulted in the identification of objects observed in the black level criteria. However, the next step of using regional minima results shows that the exudates in the area was not segmented as an object. Therefore the process of using regional minima can be replaced by other methods to better visualize the exudates
3. The best accuracy results were directly proportional to the number of correctly identified images obtained in the specified backpropagation structure and achieved an accuracy of 90.90%. The highest accuracy values were obtained with 10 correctly classified images from the 11 images tested.

REFERENCES

Akram, M. U. et al., 2013. Detection and classification of retinal lesions for grading of diabetic retinopathy. *Computers in Biology and Medicine, Elsevier,* Volume 45, p. 162.

American Diabetes Assosiation, 2010. Diagnosis and Classification of Diabetes Mellitus. *Diabetes Care,* 33(1), p. 562.

Dedeh, M., 2016. Image of Ruostejarvi.org. *Diabetes and Blindness*, 9 October.

Ekanita, D., 2004. Operasi morfologi pada suatu berkas citra monokrok*.BMP menggunakan perangkat lunak Matlab versi 6.5. In: *Skripsi.* Yogyakarta: Universitas Sanata Darma, pp. 33-35.

Hadinegoro, Ahmad, N. & Arifyanto, 2012. Metode Histogram Equalization untuk Perbaikan Citra Digital. *Semantik,* p. 440.

Kho, B., 2018. Ilmu Management Industri. *Pengertian Histogram dan Cara Membuatnya*, Januari, pp. 1-2.

Lusiana, Hartono, B. & Veronica, 2014. Analisa Teknik Adaptive Histogram Equalization dan Contrast Stretching untuk Perbaikan Kualitas Citra. *Teknologi Informasi Dinamik,* p. 3.

M. Usman Akram, d., 2013. Detection and classification of retinal lesions for grading of diabetic retinopathy. *Computers in Biology and Medicine, Elsevier,* Volume 45, p. 162.

Manullang, Y. R., Rares, L. & Sumual, V., 2015. Prevalensi Retinopati Diabetik Pada Penderita Diabetes Melitus Di Balai Kesehatan Mata Masyarakat (Bkmm) Propinsi Sulawesi Utara Periode Januari – Juli 2014.

Murinto, Putra, W. P. & Handayaningsih, S., 2008. Analisis perbandingan histogram equalization dan model Logarithmic Image Processing (LIP) untuk image enhancement. *Informatika,* 2(2), pp. 4-6.

Prasetyo, E., 2012. *Pengolahan Citra Digital dan Aplikasinya menggunakan Matlab.* s.l.:Teknik Informatika.

Singh, N. & Tripathi, R. C., 2010. Automated Early Detection of Diabetic Retinopathy Using Image Analysis Techniques. *International Journal of Computer Applications,* 8(2), p. 4.

Stitt, A. W. et al., 2015. The progress in understanding and treatment of diabetic retinopathy. In: *Progress in Retinal and Eye Research.* Northern Ireland, UK: s.n., p. 5.

Tjandrasa, H., Putra, R. E., Wijaya, A. Y. & Arieshanti, I., 2013. Classification of Non-Proliferative Diabetic

Retinopathy Based on Hard Exudates sing Soft Margin SVM. *IEEE,* p. 278.

WHO, 2016. *Global Report On Diabetes,* France: WHO Library Cataloguing-in-Publication Data.

Woods, Gonzalez, R. C. & Richard, E., 2004. *Digital Image Processing Second Edition.* New York: Prentice Hall.

Yun, W. L. et al., 2008. Identification of different stages of diabetic retinopathy using retinal optical images. *Information Sciences, ScienceDirect,* 178(2008), p. 1.